BIOCHEMISTRY
including biophysical chemistry & molecular biology

Accelerated Publication

pubs.acs.org/biochemistry

Cation-π Interactions in Lipocalins: Structural and Functional Implications

Oktay K. Gasymov,* Adil R. Abduragimov, and Ben J. Glasgow*

Departments of Pathology and Ophthalmology and Jules Stein Eye Institute, University California at Los Angeles, California 90095, United States

Supporting Information

ABSTRACT: The cation-π interaction impacts protein folding, structural stability, specificity, and molecular recognition. Cation-π interactions have been overlooked in the lipocalin family. To fill this gap, these interactions were analyzed in the 113 crystal and solution structures from the lipocalin family. The cation-π interactions link previously identified structurally conserved regions and reveal new motifs, which are beyond the reach of a sequence alignment algorithm. Functional and structural significance of the interactions were tested experimentally in human tear lipocalin (TL). TL, a prominent and promiscuous lipocalin, has a key role in lipid binding at the ocular surface. Ligand binding modulation through the loop AB at the "open" end of the barrel has been erroneously attributed solely to electrostatic interactions. Data revealed that the interloop cation-π interaction in the pair Phe28−Lys108 contributes significantly to stabilize the holo-conformation of the loop AB. Numerous energetically significant and conserved cation-π interactions were uncovered in TL and throughout the lipocalin family. Cation-π interactions, such as the highly conserved Trp17−Arg118 pair in TL, were educed in low temperature experiments of mutants with Trp to Tyr substitutions.

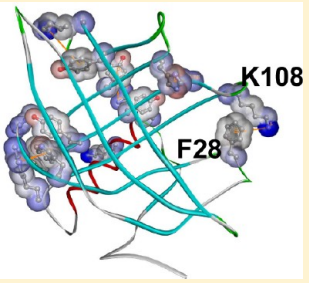

Cation-π interactions describe attraction between the positive charge of cations with the local negative charge produced by the electron-rich π system of arenes. These interactions occur with simple ions such as Li^+ to more complex organic structures as acetylcholine or positively charge groups of the side chains of the amino acid residues (Lys and Arg) and the π systems (in proteins, side chains of Phe, Tyr, and Trp). Cation-π interactions are important noncovalent forces in protein folding, stability, molecular recognition, etc.[1−5] Quantitative analysis of cation-π interactions in proteins established their energetically significant contributions in many aspects of protein functioning.[3] A prominent example is the binding of the neurotransmitter, acetylcholine. Acetylcholine directly interacts with Trp residues of the nicotinic acetylcholine receptor and acetylcholinesterase.[6,7] The mechanism is still underappreciated in ligand binding for many proteins.[3,8] In lipocalins the study of cation-π interactions has been limited to two siderocalins, the neutrophil gelatinase-associated lipocalin (NGAL) and extracellular fatty acid binding protein (Ex-FABP). The analysis was restricted to the cation-π interaction in ligand recognition, that is, only between ligand and protein side chains.[9,10] Here we will demonstrate that cation-π interactions within the protein can modulate ligand binding in a different way by stabilizing holo-form conformations in lipocalins. 113 crystal and solution structures of the proteins from the lipocalin family were analyzed for the cation-π interactions. Classification was based on the character of the interaction as well as the conserved structural regions.

The lipocalins whose membership extends to both eukaryotes and prokaryotes are best known as ligand-binding proteins. Despite the low sequence homology among the members of the family, the tertiary structures of the lipocalins are highly conserved. Human tear lipocalin (TL), also known as von Ebner's gland protein, is an archetypical ligand binding member of the lipocalin family.[11] The enhanced promiscuity of TL for lipids is derived from structural plasticity and a large mouth as determined by site-directed tryptophan fluorescence (SDTF).[12−14] X-ray crystallography of TL is concordant with the SDTF derived solution structure.[15] TL scavenges an array of lipid contaminants from the corneal surface to prevent lipid induced dry spot formation,[16,17] solubilizes lipids in tears,[12] removes harmful lipid oxidation products,[18] transports sapid molecules in saliva,[19] and traps microbial siderophores.[20]

In tears, TL is the major lipid binding protein and found complexed with an array of endogenous ligands, such as fatty acids, alkyl alcohols, glycolipids, phospholipids, and cholesterol.[21,22] With the second highest concentration of any protein in tears (~75 μM) and dissociation constants in the low micromolar range for most ligands, TL overshadows other putative ligand binding/transport proteins, for example, phospholipid binding protein.[23] Therefore, in tears, TL is positioned as the principal chaperone to modulate lipid trafficking, distribution, and clearance in the ocular surface interfaces. Virtually every function assigned to TL has been associated with various types of ligand binding. Therefore, molecular mechanisms that impact ligand binding are functionally relevant. Progress has been made on the specific mechanistic features of ligand binding to TL.[12−14,24−30] In the binding

Received: February 29, 2012
Published: March 22, 2012

   dx.doi.org/10.1021/bi3002902 | *Biochemistry* 2012, 51, 2991−3002

cavity, fatty acids are predominantly oriented with the hydrocarbon tail buried in the cavity and the carboxyl group at the calyx mouth.[29,31] A SDTF application shows bound fatty acid assumes multiple positions in the cavity in solution rather than the single position observed in the crystal environment. The binding energy landscape has demonstrated an asymmetric distribution of ligand position in the cavity.[13] Two independent methods have confirmed that residues in the loops AB and GH of TL are directly involved in ligand binding. In the loop AB the protonation state of Glu27 triggers conformational shifts between holo and apo-TL. Lys 108 is believed to stabilize the holo-conformation of the loop AB exclusively by the electrostatic interaction with Glu27.[26,30]

We carefully inspected the crystal structures of apo- and holo-TL and uncovered several cation-π interactions. In contrast to apo-TL, the cation-π interaction between Lys108 and Phe28 stabilizes the holo-conformation of the loop AB. This interaction was previously overlooked.[26,30] One of the most conserved Trp−Arg interactions in the entire lipocalin family (Trp of the strand A and Arg of the C-end of the strand H) was described as an aromatic-amine, but appears cation-π in origin.

EXPERIMENTAL PROCEDURES

A Cation-π Interaction: Observation and Calculation of the Energy. The crystal and solution structures of proteins from the lipocalin family (total of 113 structures) including that of apo- and holo-TL (PDB files, 1XKI and 3EYC (chain A), respectively) were analyzed for cation-π interactions. A computer program CAPTURE (Cation-π Trends Using Realistic Electrostatistics) (Web site: capture.caltech.edu) was used to calculate energetics of the cation-π interactions. Description of the program and details of the calculation can be found in ref 3. For TL, Discovery Studio 3.1 (Accelrys Software Inc.) was used to identify and visualize all π-interactions (cation-π, $\pi-\pi$, $\pi-\sigma$). The software uses the geometric restrictions, which are described in the manual.

Electrostatic Potential Calculations. Electrostatic potentials of the 4-methylphenol and 4-methylphenolate, which represent the Tyr side chains in neutral and ionized states, respectively, were calculated using the ArgusLab software.[32] In calculations, the side chains atoms of the Tyr beyond the $C^{\beta}H_2$, substituted for $C^{\beta}H_3$, were deleted. To obtain the electrostatic potential-mapped electron density surfaces, ground state electron densities and electrostatic potentials were calculated using the ZINDO Hamiltonian. The electron-density distributions are shown with color-contour representations.

Mutagenesis and Plasmid Construction. The cDNA of TL in PCR II (Invitrogen)[33] was used as a template to clone the TL gene spanning bases 115−592 of the previously published sequence[34] into pET 20b (Novagen, Madison, WI). Flanking restriction sites for NdeI and *Bam*HI were added to produce the native protein sequence but with the addition of an initiating methionine.[35]

To examine the influence of the conserved Trp17 on the cation-π interaction, we constructed TL mutants W17Y and W17F with oligonucleotides (Universal DNA) using the previously published method of introduction of a point mutation by sequential PCR steps as previously described.[28]

Expression and Purification of Proteins. The wild-type and the mutant plasmids were transformed in *Escherichia coli* BL 21 (DE3) and cells were cultured, and protein was expressed as indicated by the manufacturer's protocol (Novagene). Cell lysis and protein purification were performed as described previously.[36] Purity of the proteins was verified by SDS tricine gel electrophoresis.[21] The protein concentration were determined using molar extinction coefficient ε_{280} = 13 760 M^{-1} cm^{-1}.[37] For the mutant protein, W17Y, the molar extinction coefficient was calculated to be 9550 M^{-1} cm^{-1}.

Absorption Spectroscopy. UV absorption spectra were measured at 295 K and 77 K temperatures using Shimadzu UV-2400PC spectrophotometer. A minor contribution of the light scattering to the absorption spectra was corrected by plotting the log of absorbance of the solution versus the log of the wavelength and extrapolating the linear dependence between these quantities in the range 330−390 nm to the absorption range 240−330 nm. In absorption as well as CD (described below) measurements, glycerol/buffer (1:1) mixtures were used as glass-forming matrices for the protein solution. 10 mM sodium phosphate (pH 7.3) was mixed with UV-grade glycerol. The same solutions were used for the measurements at 295 K. To obtain high quality glasses that minimize light scattering, the absorption spectra were measured using a demountable cell with a path length of 0.2 mm.

CD Spectral Measurements at 295 K and 77 K. Far-UV CD spectra were recorded (Jasco 810 spectropolarimeter, 0.2 mm path length) using a protein concentration of 1.2 mg/mL. Eight scans from 190 to 260 nm were averaged. Near-UV CD spectra were recorded (0.2 mm path length) using protein concentration about 50 mg/mL. At least 25 spectra were averaged for the near-UV CD spectra at 77 K. To ensure that spectra delineating Tyr ionization at 77 K are free of artifacts, two identical sample preparations were made and measured for the near-UV CD and absorption measurements of W17Y. The CD spectra were recorded in mdegrees and converted to molar absorbance units ($\Delta\varepsilon$, M^{-1} cm^{-1}). To be consistent with the literature, the far-UV CD spectra are shown in per residue values.

pH-Titration Experiments Monitored by Steady-State Fluorescence Spectroscopy. Steady-state fluorescence measurements were made on a Jobin Yvon-SPEX (Edison, NJ) Fluorolog tau-3 spectrofluorometer. The bandwidths for excitation and emission monochromators were 3 nm. The excitation λ was 285 nm. Protein solutions of about 0.1 OD in a 5 mm path length cell were analyzed. All spectra were obtained from samples in 5 mM sodium phosphate (pH 7.5−5.5) or 15 mM sodium citrate (pH 4.0−2.0) at room temperature. To be consistent with a low temperature study design, all protein solutions contained 50% glycerol. The fluorescence spectra were corrected for light scattering from buffer. Each fluorescence value at λ = 340 nm was determined as an average of five measurements. Data were analyzed with the assumption that pH-dependent changes in fluorescence are driven by the ionization state of Tyr. Ionized Tyr residues exhibit red-shifted fluorescence emission (λ_{max} ~ 340 nm) compared to that of neutral Tyr (λ_{max} ~ 305 nm). pH titration data were analyzed by fitting the function derived from the Henderson−Hasselbalch equation for multiple titratable groups:[38]

$$F_{obs}^{340nm} = F_{min}^{340nm} + \sum_i \frac{\Delta F_i^{340nm} \times 10^{(pH-pK_i)}}{1 + 10^{(pH-pK_i)}}$$

where $F_{obs}^{340\ nm}$ is the observed fluorescence intensity at 340 nm at any pH; $F_{min}^{340\ nm}$ is the fluorescence intensity at the minimum

dx.doi.org/10.1021/bi3002902 | *Biochemistry* 2012, 51, 2991−3002

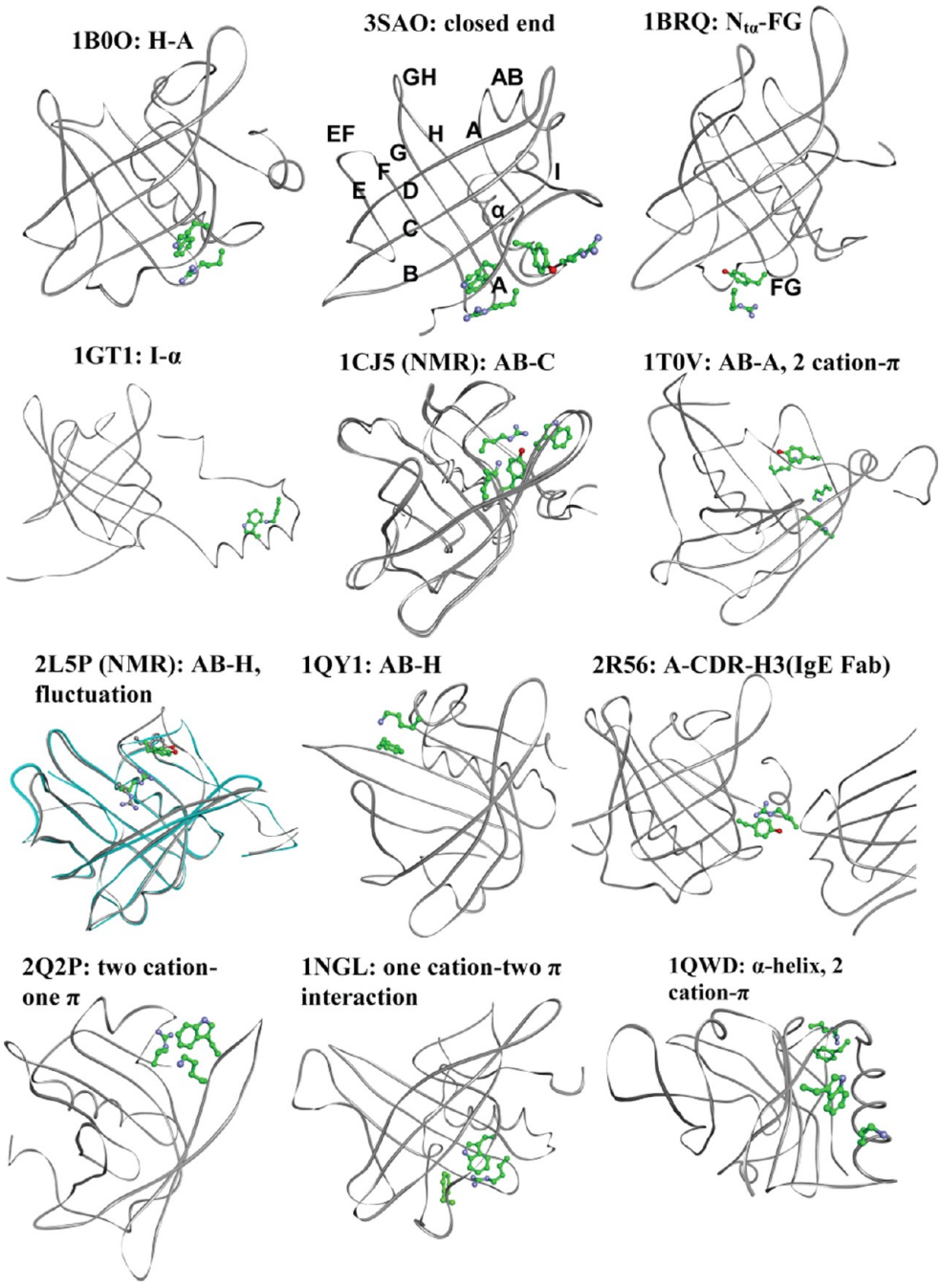

Figure 1. The ribbon diagrams of the proteins from the lipocalin family show the distribution of cation-π interactions. Single and double capital letters show identities of the β-strands and the loops, respectively. The localization (highlighted with bold letters in Table 1) and/or description of the cation-π interaction are provided after the PDB code. The designations of the PDB codes are shown in Table 1.

pH value; $\Delta F_i^{340\ nm}$ is the fluorescence intensity difference due to titration of the particular group assigned by subscript. This equation assumes a noninteracting model with a rapid equilibrium between protonated and unprotonated groups. Data obtained for both W17F and W17Y were fit simultaneously (pK_i values were treated as global parameters) to the above shown formula using OriginPro 8 software with the nonlinear least-squares method. Two pK_a parameters were needed to describe the titration curve.

RESULTS

Energetic Evaluation of the Cation-π Interactions in the Proteins of the Lipocalin Family. Overall, 113 available crystal and solution structures of the proteins from the lipocalin family were analyzed to detect energetically significant cation-π interactions using the program CAPTURE (Table S1, Supporting Information). Some proteins have more than one crystal structure; for example, porcine odorant binding protein has eight crystal structures. Data indicate that many lipocalins possess numerous energetically significant (electrostatic interaction, $E_{es} < -2.0$ kcal/mol) cation-π interactions. Representative cation-π interactions of lipocalins and calculated energies are shown in Figure 1 and Table 1. It is evident that cation-π interactions are not localized in one region but widely distributed in the protein structures. As will be shown below,

dx.doi.org/10.1021/bi3002902 | Biochemistry 2012, 51, 2991−3002

Table 1. Representative Cation-π Interactions in the Proteins from the Lipocalin Family Listed by Protein Data Bank Identification (PDB ID)[a]

PDB ID	origin	ligand	cation-π pair	location/subunit[b]	E^c (es)	E^d (vdw)
		Tear Lipocalin				
1XKI	human		Arg137-Tyr100	αI-G	−3.05	−2.34
			Arg118-Trp17	H-A	−2.81	−3.02
			Lys70-Tyr77	D-E	−3.99	−1.40
3EYC	human	1,4-butanediol	Arg137-Tyr87	α-F/A	−1.86	−1.14
			Arg137-Tyr100	α-G/A	−2.75	−3.38
			Arg118-Trp17	H-A	−2.35	−3.28
			Arg118-[e]Tyr17	H-A	−4.15	−3.39
			Arg118-[e]Phe17	H-A	−4.27	0.04
			[f]Lys108-Phe28	H-AB	−2.75	−0.68
			Lys108-Trp28	H-AB	−4.39	−0.81
		Odorant Binding Protein				
1GT1	bovine	anthracen-1-ylamine	**Lys143-Trp133**	I-α/A	−7.82	−1.32
		Retinol Binding Protein from Plasma				
1BRQ	human		**Arg19-Tyr111**	$N_{t\alpha}$-FG	−2.05	−3.05
			Arg60-Tyr173	C−C_t	−2.01	−0.99
			Arg139-Trp24	H-A	−4.62	−4.21
			Lys85-Trp105	E-F	−9.41	−0.59
			Lys89-Trp91	E-E	−3.59	−0.78
		Beta-lactogloblin				
1B0O	bovine	palmitic acid	**Arg124-Trp19**	H-A	−5.10	−1.52
2Q2P	[RN]bovine		**Arg40-Trp61**	AB-C	−2.45	−0.41
			Arg124-Trp19	H-A	−4.04	−3.97
			Lys60-Trp61	C−C	−6.00	18.61
2R56	bovine	human IgE Fab Fragment and dodecyl-beta-D-maltoside	**Arg101-Tyr20**	CDR-H3/H-A/A[g]	−2.71	−2.95
			Arg124-Trp19	H-A/A	−4.05	−2.86
1CJ5	bovine, pH 2.0, NMR		**Arg40-Trp61**	AB-C/m1	−2.42	−0.99
			Arg124-Trp19	H-A/m1	−3.43	−1.91
			Arg40-Trp61	AB-C/m2	−1.55	−1.16
			Arg124-Trp19	H-A/m2	−2.77	−0.64
			Lys141-Tyr102	α-G/m2	−2.50	−0.77
			Lys69-Tyr42	C-AB/m6	−2.36	−0.46
		Bilin Binding and Engineered Lipocalins				
1T0V	butterfly, [EN]FluA, NMR		Arg58-Trp129	C−H/m1	−3.57	−0.96
			Lys31-Tyr39	A-AB/m1	−4.73	−0.13
			Lys41-Trp27	AB-A/m1	−2.27	−0.43
			Lys25-Trp44	A-B/m3	−3.11	−0.86
			Arg58-Trp27	C-A/m4	−3.61	−2.18
			Lys96-Tyr85	F-E/m4	−3.19	−1.23
			Lys159-Tyr32	αI-A/m4	−3.30	−0.95
			Lys25-Trp27	N_t-A/m6	−3.22	−0.34
			Lys121-Tyr3	GH- N_t/m10	−2.39	−0.44
		Neutrophil Gelatinase-Associated Lipocalin (NGAL, Lipocalin 2) and Engineered NGALs				
1NGL	human, NMR		**Arg141-Phe28**	H−N_t	−2.93	−1.44
			Arg82-Trp80	D-D	−1.87	−1.52
			Arg141-Trp32	H-A	−6.94	3.37
		Major Urinary Protein				
1QY1	mouse	2-isobutyl-3-methoxypyrazine	Arg122-Trp19	H-A	−3.94	−4.10
			Lys31-Phe114	AB-H	−3.07	−0.17
		Bacterial Lipocalin				
1QWD	*E. coli*		**Arg135-Phe164**	GH-αI/A	−2.27	−1.91
			Arg52-Phe53	AB-AB/B	−2.77	−1.58
			Arg135-Phe164	GH-αI/B	−2.25	−1.80
			Arg38-Tyr125	N_t-FG/B	−1.02	−2.40
			Arg101-Tyr17	D-N_t/B	−3.79	−3.18
			Arg143-Trp43	H-A/A	−4.29	−4.94
			Arg143-Trp43	H-A/B	−4.18	−5.01
			Lys105-Tyr113	E-F/B	−2.24	−0.49
			Lys152-Trp171	α-I/A	−3.48	−0.72
			Lys77-Trp86	C-D/B	−4.06	−0.95

dx.doi.org/10.1021/bi3002902 | *Biochemistry* 2012, 51, 2991−3002

Table 1. continued

PDB ID	origin	ligand	cation-π pair	location/subunit[b]	E^c (es)	E^d (vdw)
		Bacterial Lipocalin				
			Lys152-Trp171	α-I/B	−3.97	−0.80
		Siderocalin Extracellular Fatty Acid-Binding Protein (Ex-FABP)				
3SAO	chicken		Arg135-Phe98	αI-G/B	−3.94	−2.14
			Arg118-Tyr13	Hα-A/B	−1.24	−2.41
			Arg59-Trp61	D-D/B	−5.39	−2.43
			Arg116-Trp12	H-A/B	−3.19	−4.69
		Lipocalin 12				
2L5P	rat, NMR		Lys48-Tyr137	$N_{t\alpha}$-FG/m1	−1.98	−1.11
			Lys165-Trp164	Hα-Hα/m1	−1.23	−1.28
			Arg116-Tyr103	E-D/m2	−4.18	−3.97
			Arg162-Trp53	H-A/m2	−4.33	−3.43
			Arg162-Trp53	H-A/m3	−4.17	−1.45
			Arg156-Tyr63	H-AB/m3	−2.17	−0.89

[a]See Table S1 for the complete list of the proteins. [b]β-strands, one letter, loops two letter, α-main α-helix; /letter, subunit or model number (NMR). [c]Electrostatic interaction. [d]van der Waals interaction. [e]According to the software CAPTURE, the cation-π interactions in apo-forms of these mutants are not energetically significant. [f]For Lys 108 conformation with (Chi 1 = −172.10°, and Chi 2 = 175.34°; 24% populated); $N_{t\alpha}$ - N-terminal α helix; C_t - C-terminal; ^{RN} - reverse native. [g]CDR-H3, CDR (complementary-determining region) loop of the IgE Fab participate; ^{EN}-engineered lipocalin; N_t - N-terminal. The cation-π interactions represented in Figure 1 are shown in bold-faced letters. Unless otherwise stated PDB files were analyzed with the deposited side chain rotamers only. Structures were not modified to remove unfavorable interactions (positive E_{vdw}).

cation-π interactions link all SCRs (SCR, structurally conserved region) of the lipocalin family.

Detection and Energetic Evaluation of the π-Interactions in apo- and holo-TL. The ribbon diagrams of the crystal structures of TL in apo- and holo-forms as well as the stick models of the amino acid side chains involved in π-interactions are depicted in Figure 2. The software uses geometric restrictions (distance and angle) to predict the π-interactions. Although the cation-π interaction is not detected for residues Arg90 and Tyr97, these residues are within hydrogen bonding distance in holo-TL (Figure 2B, yellow double-headed arrow). Such is not the case in apo-TL. The relevant distances between different pairs of the amino acid residues are shown in Table S2, Supporting Information. The cation-π interactions are located inside as well as outside of the binding cavity. In some cases, the apo-holo transition results in the formation of new cation-π interactions (between Phe28 of the loop AB and Lys108 of the β-strand H) as well as modification of existing ones (between Arg137 and Tyr100 or Tyr 87) (Figure 2). Quantitative evaluation indicates that the predicted cation-π interactions are energetically significant (Table 1). The software CAPTURE uses energy-based rather than geometry-based criteria and, therefore, only accounts for the pairs in which $E_{es} \leq -1.0$ kcal/mol. If E_{es} contribution is ≤ -2.0 kcal/mol, then the pair is considered to have a significant cation-π interaction.[3] Previously, SDTF was applied to TL to evince the ligand-binding mechanism.[26] In this method, amino acid residues were sequentially replaced with Trp. The mutation of Phe28 to Trp28 did not diminish but rather enhanced the cation-π interaction. The magnitude of electrostatic contribution increased to −4.39 kcal/mol with Trp in contrast to −2.75 kcal/mol observed with Phe (Table 1). Therefore, the ligand binding mechanism is intact in the mutant F28W.

The role of Trp17 in the cation-π interaction between residues Arg118 and Trp17 is multifarious. In apo-TL, the mutation of Trp to either Phe or Tyr disrupts the interaction. However, in holo-TL, both mutations exhibit significantly enhanced cation-π interaction (Table 1). Analogous Trp−Arg interactions localized at the closed-end of the barrels of the

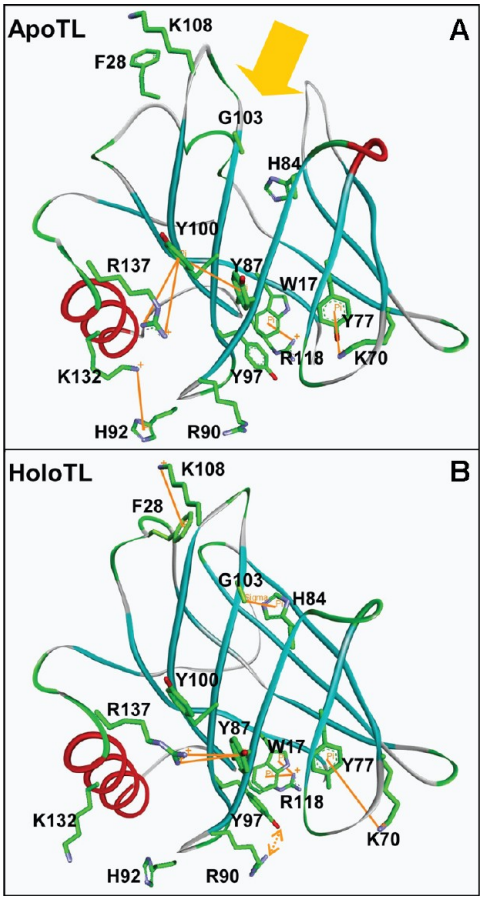

Figure 2. π interactions in the crystal structures of TL in apo- (PDB: 1XKI) (A) and holo-forms (PDB: 3EYC) (B). The residues involved in π-interactions as well as the hydrogen bond between R90 and R118 are shown in stick representation. π-interactions were detected by the software, Discovery Studio 3.1. Color coding: green for carbon atoms, red for oxygens, and blue for nitrogens. The large yellow arrow indicates the entrance the binding cavity. See Figure 1 for the guidance of locations of the β-strands and the loops.

dx.doi.org/10.1021/bi3002902 | *Biochemistry* 2012, 51, 2991−3002

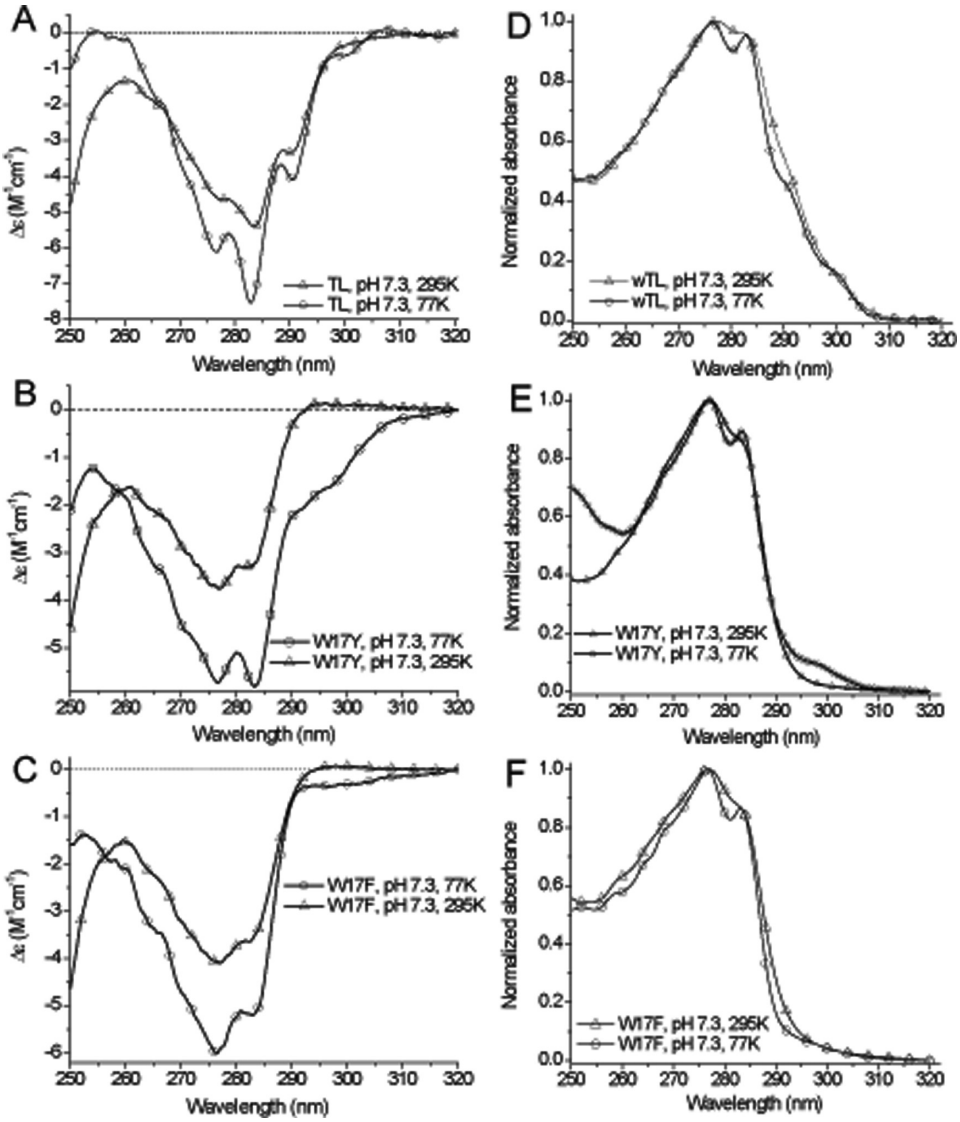

Figure 3. Molar near-UV CD and normalized absorption spectra of TL and its mutant at 295 K and 77 K. (A–C) near-UV CD spectra. (D–F) absorption spectra. To ensure spectral differences were free of artifacts, three identical sample preparations at 77 K and 295 K were used.

proteins are conserved not only in the lipocalin family but also in a larger protein superfamily, calycins.[39] The calculations of the conserved Trp–Arg interactions in many proteins from the lipocalin family reveal cation-π interactions (Table S1, Supporting Information). A number of proteins from the calycins family show Trp to Tyr or Phe substitution. Previously, Trp17 to Tyr and Phe mutations were assessed in TL with regard to ligand binding and protein stability.[28]

Low Temperature near-UV CD Spectroscopy. Because the Trp–Arg interaction appears to be the most conserved in the lipocalin family, a series of experiments were performed to further evaluate its role in TL, applicable to the lipocalin family.

Compared with room temperature, low-temperature near-UV CD exhibits higher resolution in the spectra of aromatic residues.[40] To assess the environment of aromatic residues in TL as well as the secondary structure, low-temperature CD experiments were performed in the near and far-UV regions. In the far-UV region, essentially the spectrum of TL at 77 K has the same characteristics as that obtained at 295 K, but has a narrower width (Figure S1, Supporting Information). Thus, the secondary structure of TL is intact at 77 K.

Near-UV CD spectra of TL and its mutants (W17Y and W17F) at 77 K and 295 K are shown in Figure 3A–C. The fine features for the spectra at 77 K are evident. All CD spectra at 77 K show higher intensity. The vibronic band at 290.6 nm belongs to the 0–0 L_b of Trp17. The vibronic bands at positions 282.2 and 276.8 nm are derived from the L_b bands of Trp17 and five Tyr residues.

Low Temperature Absorption Spectroscopy. The absorption spectrum of W17Y (Figure 3E) displays well-resolved vibronic bands at 283.3 and 276.6 nm, which correspond to the 0–0 and 0 + 800 cm^{-1} transitions of L_b band, respectively.[40,41] Surprisingly, in the CD spectra, the mutant W17Y that lacks Trp displays a new shoulder around 298 nm at 77 K but not at 295 K (Figure 3B). However, the mutant W17F does not show this feature (Figure 3C) indicating that the shoulder around 298 nm at 77K is specific to Tyr at position 17. The absorption spectra of TL and its mutants at 77 K and 295 K corroborate the CD results (Figure 3D–F). As in the case of the CD experiments, the absorption spectra at 77 K display pronounced vibronic bands. The absorption spectrum of W17Y at 77 K, but not at 295 K,

dx.doi.org/10.1021/bi3002902 | *Biochemistry* 2012, 51, 2991–3002

displays a distinct shoulder at about 298 nm and below 260 nm (Figure 3E). These unique features result from ionization of Tyr17 at 77 K. The red shift of Tyr can be observed in solutions at alkaline pH values with NATyrA (N-acetyl-tyrosine-amide) with and without glycerol (Figure S2a, Supporting Information). Glycerol minimally decreases the pH of buffer, by about 0.3 pH units. In addition, the absorption spectra of W17Y and W17F at pH 9.1 do not display signs of ionization of Tyr at room temperature (Figure S2b, Supporting Information).

Fluorescence pH Titration Experiments. The pK_a value of the side chain of Tyr is significantly shifted in the excited state.[42] To detect if the excited state pK_a value of Tyr17 is shifted compared with that of the other five Tyr residues in TL, fluorescence pH titration experiments were performed with mutants W17F and W17Y (Figure 4A,B). Results indicate that

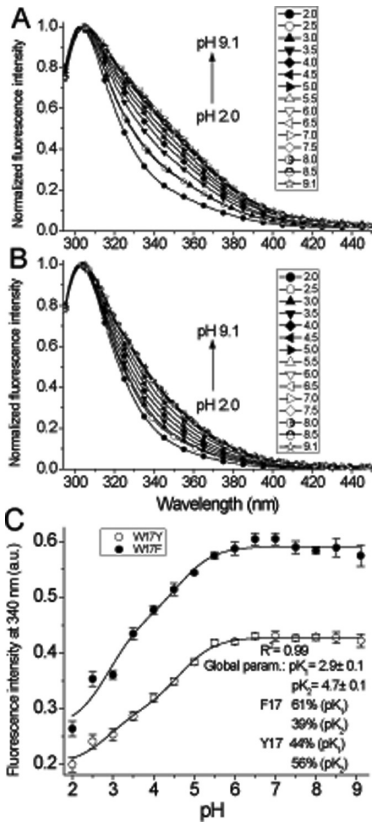

Figure 4. Fluorescence pH-titration of Trp-less mutants of TL at 295 K. Fluorescence pH-titration of the mutant W17F (A) and W17Y (B). (C) Monitoring the fluorescence intensities of W17F and W17Y at wavelength of 340 nm at various pH values.

at 295 K the contributions of the tyrosinate fluorescence intensity to the total fluorescence are different between W17F and W17Y. However, pK_a values determined from the titration curves are identical (Figure 4C). Thus, excited state pK_a value of Tyr17 at 295 K is not significantly different compared with that of other Tyr residues.

DISCUSSION

Classification of the Cation-π Interactions in the Proteins of the Lipocalin Family. The quantitative examination of the cation-π interactions in the proteins of the lipocalin family (Table S1) can be summarized as follows:

Closed-End Motif. The conserved cation-π interaction at the closed end of the barrel between the β-strands H and A is observed in 100 structures (Figure 1, 1B0O). It is absent in bovine OBP structures, which exhibit a domain swapping mechanism in dimer formation (eight structures) (Figure 1, 1GT1) as well as in engineered lipocalins (five structures, Table S1). This motif links SCR1 and SCR3 from the structural classification of the lipocalin family.[11,39] The cation-π interaction between the β-stands H and A (mostly as a pair Arg-Trp) seals the end of the barrel from the solvent molecules.

N-Terminal Motif. The cation-π interaction involving the loop FG and conserved N-terminal short 3_{10}-helix is detected in 29 structures (Table S1, Figure 1, 1BRQ). This motif links SCR1 and SCR2 regions of the lipocalin family.[11,39] This interaction plays a role in positioning of the N-terminal region, which affects closure of this end of the molecule.[11]

α-Helix Motif. The cation-π interaction that involves the main α-helix (or short loop αI) is observed in 24 structures. The partners of the cation-π interactions are paired between the main α-helix and the following parts of the structure: the β-strand A (four cases), the β-strand I or the loop αI (eight cases), the β-strand G (five cases), the β-stand F (two cases), the loop Hα (one case), the loop GH (one case), the C-terminal part (four cases), and the loop FG (one case). As can be seen in Figure 1, these cation-π interactions play an important role in fixing main α-helix positions relative to the barrel. Interestingly, the bacterial lipocalin uses two cation-π interactions located at the both ends of α-helix (Figure 1, 1QWD) to fix its position.

C-Terminal Motif. The cation-π interaction involving C-terminal and the β-strand C is observed in 22 structures (Table S1, Supporting Information). These interactions participate to attach the C-terminal end of the lipocalins to the barrel.

Loop Motif. The cation-π interaction involving the loops (not including the loops FG and αI) is observed in 22 structures. The partners of the cation-π interactions are paired between the loop AB and the following β-stands: the β-strand C (two cases), the β-stand A (one case), the β-strand D (one case), the β-stand H (five cases), and the β-strand I (one case). Intraloop cation-π interactions, where the both partners are located within the same loop, are found in the following loops: the loops AB (one case), the loops EF (two cases), the loop DE (two cases), and the loop GH (three cases) (Table S1, Supporting Information). The longest loop AB of the lipocalin family plays a significant, in some cases deterministic, role in ligand binding. The cation-π interactions involving the loop AB play a significant role in fixing its particular and/or alternative conformations (Figure 1, 1CJ5, 1T0V, 2L2P, 1QY1).

Intersubunit Motif. Within oligomeric lipocalins, the cation-π interactions between subunits are detected in seven structures (Table S1, Supporting Information). The partners of the cation-π interactions are paired between the following parts of the structures: the β-strands D and D (two cases), the β-strands D and G (two cases), the β-stand D and the loop GH (one case), and the β-strands G and F (one case). The cation-π interaction is also detected in the protein−protein interaction of β-lactoglobulin (the strand A) and recombinant IgE antibody (Figure 1, 2R56 and Table 1).

Siderocalin, Ex-FABP, uses not one but two cation-π interactions at the closed-end of the barrel (Figure 1, 3SAO, Table 1) to enhance structural stability of the protein. We discovered "two cation-one π" (one aromatic side chain is sandwiched between two cations) and "one cation-two π" (one

cation is sandwiched between two aromatic side chains) interactions (Figure 1, 2Q2P and 1NGL, respectively).

The data indicate that the cation-π interactions not only link all previously identified SCRs but also reveal the new structural (α-helix and C-terminal motifs) and functional (loop- and intersubunit motifs) patterns. Thus, the cation-π interactions uncover patterns that are beyond the reach of simple sequence alignment features.

The Cation-π Interactions in Siderophore Binding with Human NGAL. Two siderocalins (NGAL and Ex-FABP) are unique exceptions for which cation-π interactions were considered in the lipocalin[9,10] and, therefore, demand special attention. Models for the structures of the NGAL in holo- and apo-forms are shown in Figure 5. As described,[9] the side chains K125, K134, and R81 have cation-π interactions with the ligand (Figure 5a). However, the identification and implications of the cation-π interactions were limited to that between the side chains of the protein and ligand. Inspection of the structures of NGAL in holo- and apo-forms with the program CAPTURE reveal that interside chain cation-π interactions are directly involved in ligand binding. Previously, amino acid residues W79, R81, F123, K125, Y132, and K134 were alleged to define the pocket for the ligand.[9] In the apo to holo transition, significant conformational rearrangements for these residues are evident (Figure 5B,C). Our calculations indicate that the cation-π interactions in pairs K125−Y132, F123−Lys134, and R81−W79 are energetically substantial enough (Table S1, Supporting Information) to stabilize the holo-conformation of the protein. This is in addition to the cation-π bonds that were posited to occur with the ligand.[9,10] An alternative holo-conformation observed with a different ligand, carboxymycobactin T (1X8U), is stabilized by the complementary cation-π in the pair R81−Y100 (Figure 5B, inset). Except for R81−W79, none of the above-mentioned pairs display cation-π bonds in the apoprotein (Figure 5B,C). Figure 5 illustrates that these concerted conformational transitions are necessary for ligand binding from both the spatial and energetic points of views. Thus, intraprotein cation-π bond formations play a critical role in siderophore binding to NGAL.

Cation-π Interactions in TL Relevant to Structural Stability and Ligand Binding. The calculations using the crystal structures of TL in apo- and holo-forms reveal several energetically significant cation-π interactions (Figure 6, Table 1). Two independent studies have provided evidence that an electrostatic interaction between the residues Glu27 and Lys108 plays pivotal role in ligand binding.[26,30] The ribbon diagrams of TL and the stick model for the side chains at positions 27, 28, and 108 are shown in Figure 6. Despite the significant conformational changes observed for position 28 of the loop AB (Figure 6A,B), both studies have overlooked the possible cation-π interaction between Lys108 and Phe28. Because of the implications for the ligand binding mechanism, the cation-π interaction between these residues merits detailed consideration. In the apo- to holo-transition, the distance between the nitrogen atom of Lys108 and the center of the phenyl ring of Phe28 decreases from 7.4 Å to 5.2 Å. In this transition, the magnitude of the electrostatic contribution for the Lys108−Phe28 interaction increases to −2.75 kcal/mol from ←1.0 kcal/mol (Figure 6 and Table 1). Thus, the pair Lys108−Phe28 has a significant cation-π interaction,[3] which belongs to the loop motif indentified for the lipocalin family.

Previously published data obtained by SDTF reveal complementary information. Among the tested single Trp

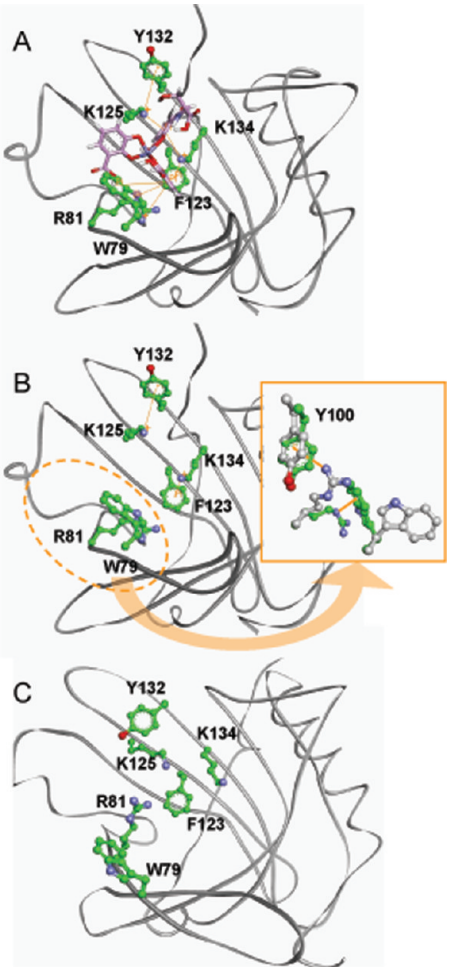

Figure 5. Cation-π interactions in NGAL relevant to ligand binding. (A) Model of the crystal structure of holo-NGAL (PDB: 1L6M) to show residues participating interside chain and side chain-ligand cation-π interactions. (B) Panel A with removed ligand to accentuate interside chain cation-π interactions that stabilize the holo-conformation. Inset: Alternative cation-π interaction of R81 that was observed in the crystal structure of NGAL with a different ligand, carboxymcobactin T. Side chains from 1L6M (chain A) are superimposed with that of 1X8U (chain B). (C) Model for the solution structure of apo-NGAL (regularized average NMR, PDB: 1NGL) to illustrate apo-conformations of the residues that lack of cation-π interactions (except the pair R81−W79). For the energies of the cation-π interactions see Table S1. Color coding for the side chains shown in ball and stick model: green for carbon atoms, red for oxygen atoms, violet-blue for nitrogen atoms, gray for carbon atoms in alternative conformation (inset, 1X8U). Carbon and hydrogen atoms of the ligand are shown in pink and white colors, respectively. See Figure 1 for the guidance of locations of the β-strands and the loops.

mutants for the loop AB, only Trp fluorescence at position 28 has displayed significant differences between apo- and holo-forms of TL in pH titration experiments.[26] The conformation of Trp28 is driven by protonation states of the neighboring residues and is stabilized by ligand binding. Moreover, the distance measurements using FRET method have indicated that in the pH induced transition, Trp28 (originally Phe28) was moved, 4.5 Å, toward the loop EF.[14] This result obtained in solution is concord with the crystal structures of TL in apo- and holo-forms.[15,30] The distance between the geometric centers of Trp28 in the apo- and holo-forms of TL in crystal structures is 4.7 Å (Figure 6c). Therefore, the apo-holo structural transition

dx.doi.org/10.1021/bi3002902 | Biochemistry 2012, 51, 2991−3002

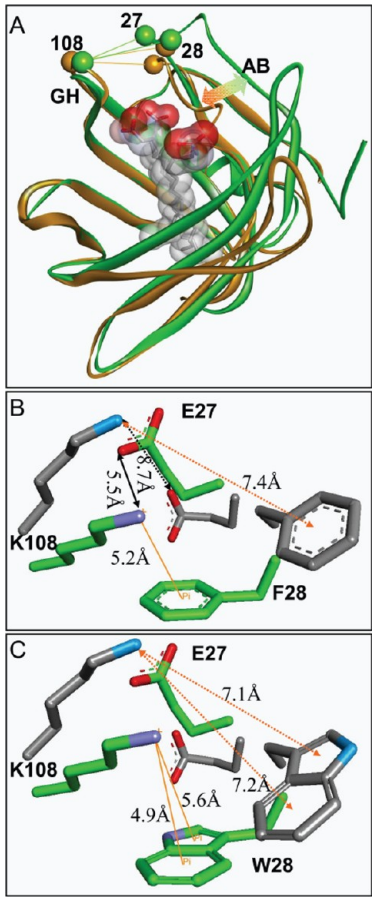

Figure 6. The cation-π interaction in ligand binding of TL. (A) Numbered and colored balls show the positions of the C^{α}-atoms of the residues 27, 28 (the loop AB), and 108 (the loop GH) in the ribbon diagrams of the crystal structures of TL in apo- (PDB: 1XKI) and holo-forms (PDB: 3EYC). Gold and green colors represent apo- and holo-TL, respectively. The double-headed arrow illustrates the displacement of the loop AB in apo-holo transition. Gold and green lines are for guidance only. Schematically, multiple positions of the palmitic acid (stick and semitransparent surface representation) in the cavity show energetically favored positions concurring with prior results.[13] See Figure 1 for the guidance of locations of the β-strands and the loops. (B) A stick model for the side chains of the residues involved in electrostatic and cation-π interactions in apo-holo transitions. Distances relevant for cation-π and electrostatic interactions are shown with gold and black arrows, respectively. For energetically insignificant interactions, the distances between the pair of the residues are illustrated with dashed lines. (C) The figure is the same as (B) but with Trp at position 28. Backbone atoms (N, C, and O) of the amino acid residues are omitted for clarity. Color coding for (B) and (C): green (holo-TL) and gray (apo-TL) for carbon atoms, violet (holo-TL) and blue (apo-TL) for nitrogen atoms, and red for oxygen atoms.

in TL is driven by the protonation state of Glu27. The mutations E27W and K108W disrupt electrostatic and cation-π/electrostatic interactions, respectively. The mutants E27W and K108W show significantly decreased affinity (K_d values ~2.5 μM and 2.7 μM, respectively) for fatty acid analogue C12SL. In contrast, the mutant F28W with an enhanced cation-π interaction (Table 1) displays higher binding affinity toward the ligand, $K_d \sim 0.4$ μM.[13] Statistically Lys-Trp cation-π pairs are more energetically significant compared to that of Lys–Phe.[3] The electrostatic potential surface of the indole group leads to a bias for the Lys–Trp cation-π interaction involving the benzene ring of the side chain of Trp.[8] Befitting these observations, the F28W mutation enhances the cation-π interaction (Figure 6 and Table 1). However, in the mutant E27W, the cation-π interaction between the residues Lys108 and Phe28 is supposed to be retained with disruption of the electrostatic interaction between Glu27 and Lys108. This mutant exhibits diminished affinity toward the ligand.[26] Therefore, the electrostatic interaction in the pair Glu27–Lys108 and the cation-π interaction in the pair Phe28–Lys108 appear to be cooperative. Apparently, ionization of Glu27 is the driving force for the conformational switch of the loop AB. It seems that the previously proposed ligand binding mechanism for TL should be modified. The "open" conformation of the loop AB in holo-protein is fixed by both the electrostatic (Glu27-Lys108) and the cation-π (Phe28-Lys108) interactions.

The Trp17–Arg118 interaction at the closed-end of the barrel is the most conserved feature (closed-end motif) in the lipocalin family.[11,39] This interaction was described as an aromatic to arginine/lysine interaction for which cation-π character was not considered.[39] However, the calculation indicates that Trp17–Arg118, as well as other homologous pairs in the lipocalin family (Table S1, Supporting Information), comprise the cation-π interaction (Figures 1, 2, and 7 and Table 1).

The effect of substitution of the conserved Trp (analogous to that of Trp17) with other aromatic residues (Tyr or Phe) varies within the lipocalin family.[28,43,44] In contrast to β-lactoglobulin and sRBP, aromatic (Phe or Tyr) substitution of Trp17 in TL results in minuscule changes in the secondary structure and stability of the protein.[28] However, the substitution of Trp17 with Cys disrupts the cation-π interaction. The mutation changes secondary structure, decreases stability of TL, and diminishes binding affinity for DAUDA.[28] The calculated energies for the cation-π interactions in mutants of TL corroborate experimental results for holo-TL (Table 1). The expressed mutant proteins of TL have some bound fatty acids.[28] Therefore, holo-forms of the proteins are appropriate for comparison.

In near-UV CD, enhanced intensities indicate that at 77 K the side chain conformations of aromatic residues are predominantly populated in fewer states than at 295 K (Figure 3A–C). At 77 K, but not 295 K, ionization of Tyr17 is observed. The observed increase in absorbance at 250 nm as well as around 298 nm (Figure 3E) confirms the deprotonation of the side chain of Tyr. Indeed, upon ionization both L_a and L_b bands of Tyr, which have maxima at 220 and 277 nm, display a red shift of about 20 nm.[45–47] In aqueous solutions, the 0–0 and 0 + 800 cm^{-1} transitions of L_b band of Tyr are observed at 282.6 and 276.3 nm, respectively.[41] A rough estimate based on the extinction coefficients of a neutral and ionized Tyr[48] indicates that about 35% of Tyr17 is ionized at 77 K (Figure 3e). The ground state pK_a value for solvent exposed as well as free Tyr is confined to the range 9.7–10.1. However, it is well documented that a nearby positive charge may significantly decrease pK_a value of residues.[49] A 2.5 unit decrease in pK_a was detected for Tyr nearby Arg.[50] The observation that about 35% of Tyr17 ionized only at 77 K indicates a shift in the conformational distribution of TL. The conformations populated at low temperature are "invisible" at room temperature.

Concordantly, the distance between the positively charged group of Arg118 and OH-group of Tyr17 decreases (Figure 7b)

dx.doi.org/10.1021/bi3002902 | *Biochemistry* 2012, 51, 2991–3002

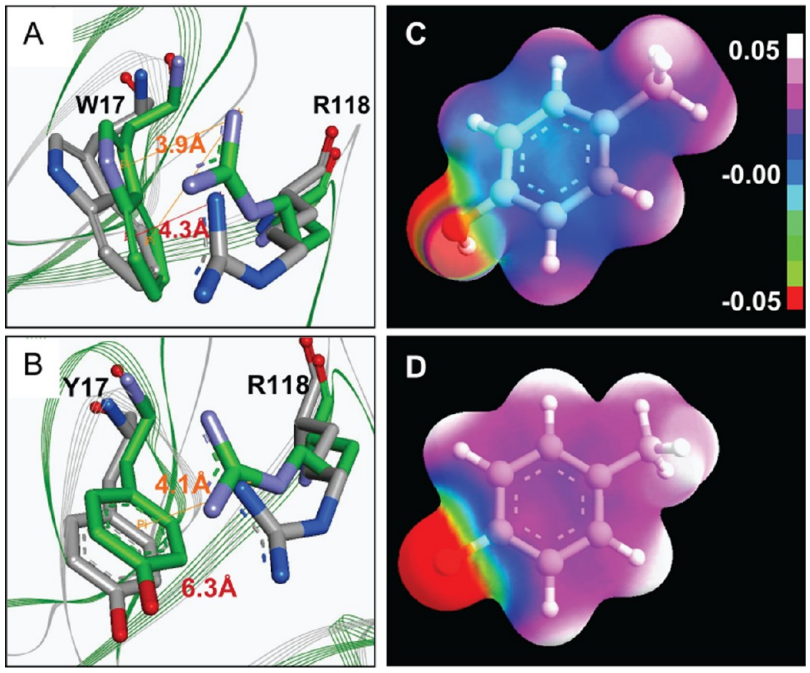

Figure 7. The cation-π interaction between residues Trp17 (or Tyr17) and Arg118, the most conserved interaction in the lipocalin family. The ribbon diagrams of the TL as well as stick models of the side chains of the proteins were generated using DS Visualizer 3.1 (Accelrys Inc.). (A) Trp17 and Arg118 residues of the apo- and holo-TL based on the crystal structures (PDB ID codes: 1XKI, gray line ribbon, and 3EYC, green line ribbon, respectively). The distances between the atoms from the respective crystal structures in apo- and holo-forms relevant for the cation-π interactions are indicated colored lines (red and yellow for apo- and holo-forms, respectively). Color scheme for apo-TL: carbon atoms, gray; nitrogen atoms, blue, oxygen atoms, red; holo-TL: carbon atoms, green; nitrogen atoms, violet, oxygen atoms, red. (B) Tyr17 and Arg118 residues of the apo- and holo-TL based on their respective crystal structures. The same software (Accelrys Inc.) was also used for the mutation in a model (Trp17 to Tyr17). The color scheme is the same as in (A). Ball and stick models superimposed with semitransparent electrostatic potential surfaces for 4-methylphenol (C) and 4-methylphenolate (D) that represent a neutral and negatively charged side chain of Tyr, respectively. Values are calculated using ArgusLab software (see Experimental Procedures for details).

for holo-TL. Ionization of Tyr transforms the character of the Tyr17−Arg118 interaction. The electrostatic potential at the center of the phenol ring is negative[8] (Figure 7c) that makes the cation-π interaction feasible with the side chain of Arg. However, the electrostatic potential in phenolate is positive (Figure 7d) and, therefore, π-system is not available for the cation-π interaction. Thus, at pH 7.3, low temperature specifically populates the conformation of TL in which the interaction between Tyr17 and Arg118 is purely electrostatic; only the $-O^-$ group of Tyr side chain participates in the interaction.

The major implication of this work is that cation-π interactions influence the selection of conformations for ligand binding in TL as well as the entire lipocalin family.

■ ASSOCIATED CONTENT

Supporting Information

Far-UV CD spectra of TL at 77 K and 295 K, absorption spectra of the TL mutants and model compound, as well as energetic evaluations of the cation-π interactions in the proteins (total of 113) from the lipocalin family are provided. This material is available free of charge via the Internet at http://pubs.acs.org.

■ AUTHOR INFORMATION

Corresponding Author

*(O.K.G.) Address: 100 Stein Plaza, Rm# B267, Los Angeles, CA 90095. Phone: (310) 825-6261. Fax: (310) 794-2144. E-mail: ogassymov@mednet.ucla.edu. (B.J.G.) Address: 100 Stein Plaza, Rm# B269, Los Angeles, CA 90095. Phone: (310) 825-6998. Fax: (310) 794-2144; bglasgow@mednet.ucla.edu.

Funding

This work was supported by U.S. Public Health Service Grants NIH EY11224 and EY00331 as well as the Edith and Lew Wasserman Endowed Professorship in Ophthalmology (B.G.).

Notes

The authors declare no competing financial interest.

■ ABBREVIATIONS

CD, circular dichroism; C12SL, spin labeled analogue of palmitic acid; DAUDA, 11-(((5-(dimethlyamino)-1-naphthalenyl) sulfonyl)amino)undecanoic acid; NATyrA, *N*-acetyl-tyrosine-amide; SDTF, site directed tryptophan fluorescence; sRBP, serum retinol binding protein; TL, human tear lipocalin

■ REFERENCES

(1) Mecozzi, S., West, A. P. Jr., and Dougherty, D. A. (1996) Cation-π interactions in aromatics of biological and medicinal interest: electrostatic potential surfaces as a useful qualitative guide. *Proc. Natl. Acad. Sci. U. S. A. 93*, 10566−10571.

(2) Ma, J. C., and Dougherty, D. A. (1997) The cation-π interaction. *Chem. Rev. 97*, 1303−1324.

(3) Gallivan, J. P., and Dougherty, D. A. (1999) Cation-π interactions in structural biology. *Proc. Natl. Acad. Sci. U. S. A. 96*, 9459−9464.

(4) Meyer, E. A., Castellano, R. K., and Diederich, F. (2003) Interactions with aromatic rings in chemical and biological recognition. *Angew. Chem., Int. Ed. Engl. 42*, 1210−1250.

(5) Xue, Y., Davis, A. V., Balakrishnan, G., Stasser, J. P., Staehlin, B. M., Focia, P., Spiro, T. G., Penner-Hahn, J. E., and O'Halloran, T. V.

(2008) Cu(I) recognition via cation-pi and methionine interactions in CusF. *Nat. Chem. Biol. 4*, 107−109.
(6) Sussman, J. L., Harel, M., Frolow, F., Oefner, C., Goldman, A., Toker, L., and Silman, I. (1991) Atomic structure of acetylcholinesterase from Torpedo californica: a prototypic acetylcholine-binding protein. *Science 253*, 872−879.
(7) Zhong, W., Gallivan, J. P., Zhang, Y., Li, L., Lester, H. A., and Dougherty, D. A. (1998) From ab initio quantum mechanics to molecular neurobiology: a cation-π binding site in the nicotinic receptor. *Proc. Natl. Acad. Sci. U. S. A. 95*, 12088−12093.
(8) Dougherty, D. A. (1996) Cation-π interactions in chemistry and biology: a new view of benzene, Phe, Tyr, and Trp. *Science 271*, 163−168.
(9) Goetz, D. H., Holmes, M. A., Borregaard, N., Bluhm, M. E., Raymond, K. N., and Strong, R. K. (2002) The neutrophil lipocalin NGAL is a bacteriostatic agent that interferes with siderophore-mediated iron acquisition. *Mol. Cell 10*, 1033−1043.
(10) Correnti, C., Clifton, M. C., Abergel, R. J., Allred, B., Hoette, T. M., Ruiz, M., Cancedda, R., Raymond, K. N., Descalzi, F., and Strong, R. K. (2011) Galline Ex-FABP is an antibacterial siderocalin and a lysophosphatidic acid sensor functioning through dual ligand specificities. *Structure 19*, 1796−1806.
(11) Flower, D. R. (1996) The lipocalin protein family: structure and function. *Biochem. J. 318* (Pt 1), 1−14.
(12) Gasymov, O. K., Abduragimov, A. R., Yusifov, T. N., and Glasgow, B. J. (2001) Site-directed tryptophan fluorescence reveals the solution structure of tear lipocalin: evidence for features that confer promiscuity in ligand binding. *Biochemistry 40*, 14754−14762.
(13) Gasymov, O. K., Abduragimov, A. R., and Glasgow, B. J. (2009) Intracavitary ligand distribution in tear lipocalin by site-directed tryptophan fluorescence. *Biochemistry 48*, 7219−7228.
(14) Gasymov, O. K., Abduragimov, A. R., and Glasgow, B. J. (2010) Excited protein states of human tear lipocalin for low- and high-affinity ligand binding revealed by functional AB loop motion. *Biophys. Chem. 149*, 47−57.
(15) Breustedt, D. A., Korndorfer, I. P., Redl, B., and Skerra, A. (2005) The 1.8-Å crystal structure of human tear lipocalin reveals an extended branched cavity with capacity for multiple ligands. *J. Biol. Chem. 280*, 484−493.
(16) Gasymov, O. K., Abduragimov, A. R., Prasher, P., Yusifov, T. N., and Glasgow, B. J. (2005) Tear lipocalin: evidence for a scavenging function to remove lipids from the human corneal surface. *Invest. Ophthalmol. Vis. Sci. 46*, 3589−3596.
(17) Glasgow, B. J., Gasymov, O. K., Abduragimov, A. R., Engle, J. J., and Casey, R. C. (2010) Tear lipocalin captures exogenous lipid from abnormal corneal surfaces. *Invest. Ophthalmol. Vis. Sci. 51*, 1981−1987.
(18) Lechner, M., Wojnar, P., and Redl, B. (2001) Human tear lipocalin acts as an oxidative-stress-induced scavenger of potentially harmful lipid peroxidation products in a cell culture system. *Biochem. J. 356*, 129−135.
(19) Blaker, M., Kock, K., Ahlers, C., Buck, F., and Schmale, H. (1993) Molecular cloning of human von Ebner's gland protein, a member of the lipocalin superfamily highly expressed in lingual salivary glands. *Biochim. Biophys. Acta 1172*, 131−137.
(20) Fluckinger, M., Haas, H., Merschak, P., Glasgow, B. J., and Redl, B. (2004) Human tear lipocalin exhibits antimicrobial activity by scavenging microbial siderophores. *Antimicrob. Agents Chemother. 48*, 3367−3372.
(21) Glasgow, B. J., Abduragimov, A. R., Farahbakhsh, Z. T., Faull, K. F., and Hubbell, W. L. (1995) Tear lipocalins bind a broad array of lipid ligands. *Curr. Eye Res. 14*, 363−372.
(22) Dean, E. W., and Glasgow, B. J. (2012) Mass spectrometric identification of phospholipids in tears and tear lipocalin. *Invest. Ophthalmol. Vis. Sci.*, Mar 6. [Epub ahead of print] PMID: 22395887.
(23) Jauhiainen, M., Setala, N. L., Ehnholm, C., Metso, J., Tervo, T. M., Eriksson, O., and Holopainen, J. M. (2005) Phospholipid transfer protein is present in human tear fluid. *Biochemistry 44*, 8111−8116.
(24) Gasymov, O. K., Abduragimov, A. R., and Glasgow, B. J. (2007) Evidence for internal and external binding sites on human tear lipocalin. *Arch. Biochem. Biophys. 468*, 15−21.
(25) Gasymov, O. K., Abduragimov, A. R., and Glasgow, B. J. (2008) Ligand binding site of tear lipocalin: contribution of a trigonal cluster of charged residues probed by 8-anilino-1-naphthalenesulfonic acid. *Biochemistry 47*, 1414−1424.
(26) Gasymov, O. K., Abduragimov, A. R., and Glasgow, B. J. (2010) pH-Dependent conformational changes in tear lipocalin by site-directed tryptophan fluorescence. *Biochemistry 49*, 582−590.
(27) Gasymov, O. K., Abduragimov, A. R., Yusifov, T. N., and Glasgow, B. J. (1998) Structural changes in human tear lipocalins associated with lipid binding. *Biochim. Biophys. Acta 1386*, 145−156.
(28) Gasymov, O. K., Abduragimov, A. R., Yusifov, T. N., and Glasgow, B. J. (1999) Binding studies of tear lipocalin: the role of the conserved tryptophan in maintaining structure, stability and ligand affinity. *Biochim. Biophys. Acta 1433*, 307−320.
(29) Gasymov, O. K., Abduragimov, A. R., Yusifov, T. N., and Glasgow, B. J. (2000) Resolution of ligand positions by site-directed tryptophan fluorescence in tear lipocalin. *Protein Sci. 9*, 325−331.
(30) Breustedt, D. A., Chatwell, L., and Skerra, A. (2009) A new crystal form of human tear lipocalin reveals high flexibility in the loop region and induced fit in the ligand cavity. *Acta Crystallogr. D Biol. Crystallogr. 65*, 1118−1125.
(31) Glasgow, B. J., Gasymov, O. K., Abduragimov, A. R., Yusifov, T. N., Altenbach, C., and Hubbell, W. L. (1999) Side chain mobility and ligand interactions of the G strand of tear lipocalins by site-directed spin labeling. *Biochemistry 38*, 13707−13716.
(32) Thompson, M. A. *ArgusLab 4.0*, Planaria Software LLC, Seattle, http://www.ArgusLab.com.
(33) Glasgow, B. J., Heinzmann, C., Kojis, T., Sparkes, R. S., Mohandas, T., and Bateman, J. B. (1993) Assignment of tear lipocalin gene to human chromosome 9q34−9qter. *Curr. Eye Res. 12*, 1019−1023.
(34) Redl, B., Holzfeind, P., and Lottspeich, F. (1992) cDNA cloning and sequencing reveals human tear prealbumin to be a member of the lipophilic-ligand carrier protein superfamily. *J. Biol. Chem. 267*, 20282−20287.
(35) Glasgow, B. J. (1995) Tissue expression of lipocalins in human lacrimal and von Ebner's glands: colocalization with lysozyme. *Graefes Arch. Clin. Exp. Ophthalmol. 233*, 513−522.
(36) Marston, F. A. O. (1987) The Purification of Eukaryotic Polypeptides Expresses in Eschericia coli, in *DNA Cloning: A Practical Approach* (Glover, D. M., Ed.), pp 59−88, IRL Press, Oxford, England.
(37) Gasymov, O. K., Abduragimov, A. R., and Glasgow, B. J. (2011) The conserved disulfide bond of human tear lipocalin modulates conformation and lipid binding in a ligand selective manner. *Biochim. Biophys. Acta 1814*, 671−683.
(38) Freedman, M. H., Lyerla, J. R. Jr., Chaiken, I. M., and Cohen, J. S. (1973) Carbon-13 nuclear-magnetic-resonance studies on selected amino acids, peptides, and proteins. *Eur. J. Biochem. 32*, 215−226.
(39) Flower, D. R., North, A. C., and Sansom, C. E. (2000) The lipocalin protein family: structural and sequence overview. *Biochim. Biophys. Acta 1482*, 9−24.
(40) Strickland, E. H. (1974) Aromatic contributions to circular dichroism spectra of proteins. *CRC Crit. Rev. Biochem. 2*, 113−175.
(41) Horwitz, J., Strickland, E. H., and Billups, C. (1970) Analysis of the vibrational structure in the near-ultraviolet circular dichroism and absorption spectra of tyrosine derivatives and ribonuclease-A at 77 degrees K. *J. Am. Chem. Soc. 92*, 2119−2129.
(42) Szabo, A. G., Lynn, K. R., Krajcarski, D. T., and Rayner, D. M. (1978) Tyrosinate fluorescence maxima at 345 nm in proteins lacking tryptophan at pH 7. *FEBS Lett. 94*, 249−252.
(43) Greene, L. H., Chrysina, E. D., Irons, L. I., Papageorgiou, A. C., Acharya, K. R., and Brew, K. (2001) Role of conserved residues in structure and stability: tryptophans of human serum retinol-binding protein, a model for the lipocalin superfamily. *Protein Sci. 10*, 2301−2316.

(44) Katakura, Y., Totsuka, M., Ametani, A., and Kaminogawa, S. (1994) Tryptophan-19 of beta-lactoglobulin, the only residue completely conserved in the lipocalin superfamily, is not essential for binding retinol, but relevant to stabilizing bound retinol and maintaining its structure. *Biochim. Biophys. Acta 1207*, 58−67.
(45) Takeuchi, H. (2011) UV Raman markers for structural analysis of aromatic side chains in proteins. *Anal. Sci. 27*, 1077.
(46) Asher, S. A., Larkin, P. J., and Teraoka, J. (1991) Ultraviolet resonance Raman and absorption difference spectroscopy of myoglobins: titration behavior of individual tyrosine residues. *Biochemistry 30*, 5944−5954.
(47) Woody, A. Y., and Woody, R. W. (2003) Individual tyrosine side-chain contributions to circular dichroism of ribonuclease. *Biopolymers 72*, 500−513.
(48) Lakowicz, J. R., Ed. (2002) *Topics in Fluorescence Spectroscopy*, Vol. 3, Kluwer Academic Publishers, New York.
(49) Harris, T. K., and Turner, G. J. (2002) Structural basis of perturbed pKa values of catalytic groups in enzyme active sites. *IUBMB Life 53*, 85−98.
(50) Sun, S., and Toney, M. D. (1999) Evidence for a two-base mechanism involving tyrosine-265 from arginine-219 mutants of alanine racemase. *Biochemistry 38*, 4058−4065.